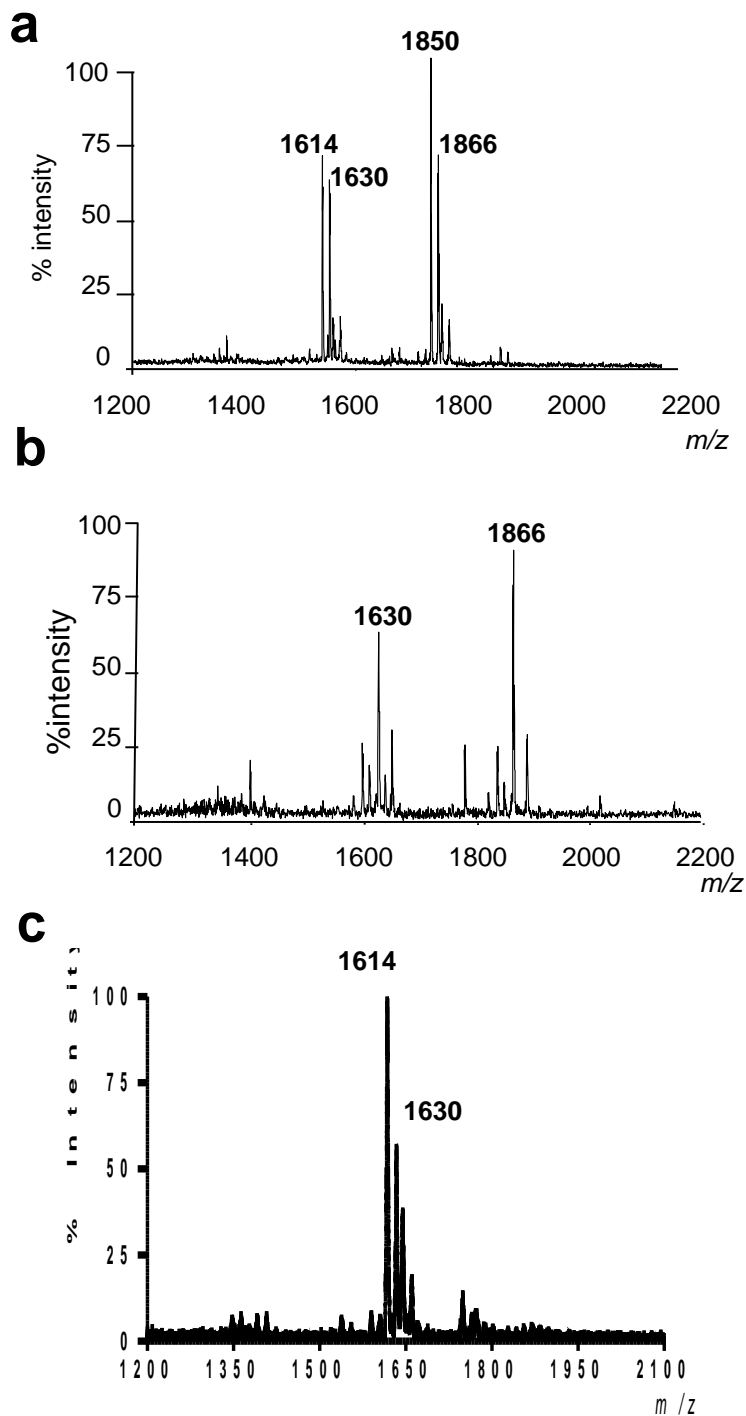


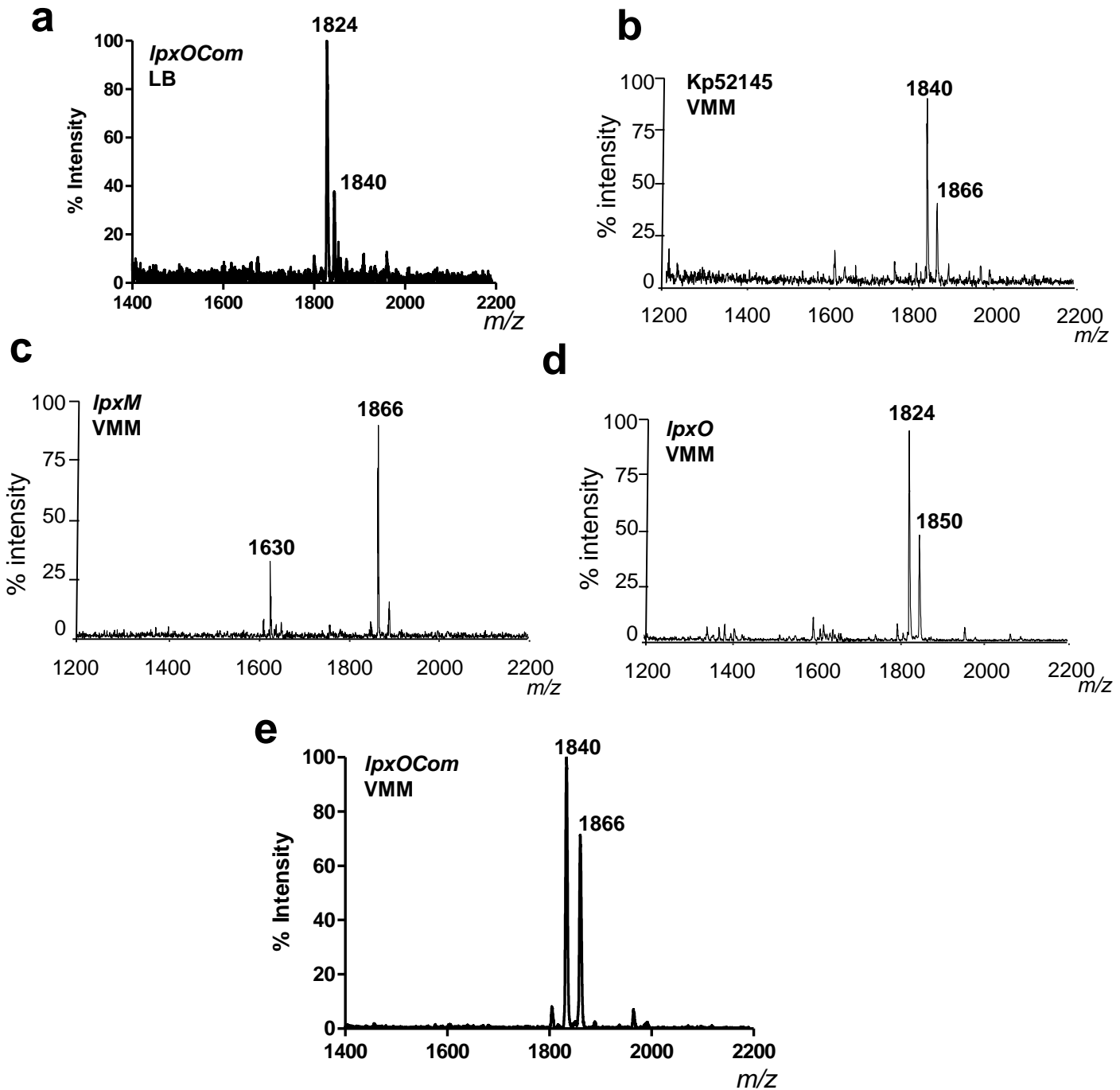
Supplementary Figure 1. Analysis of *K. pneumoniae* lipid A *in vivo*

Negative ion MALDI-TOF mass spectrometry spectra from **a.** BALF obtained of Kp52145-infected mice (lipid A was extracted using the Trizol method); **b.** lung homogenates of Kp52145-infected mice after 24 h; **c.** lung homogenates after 48 h infection. **d.**, spleen obtained of Kp52145-infected mice after 24 h In all panels results are representative from extractions from five infected animals.



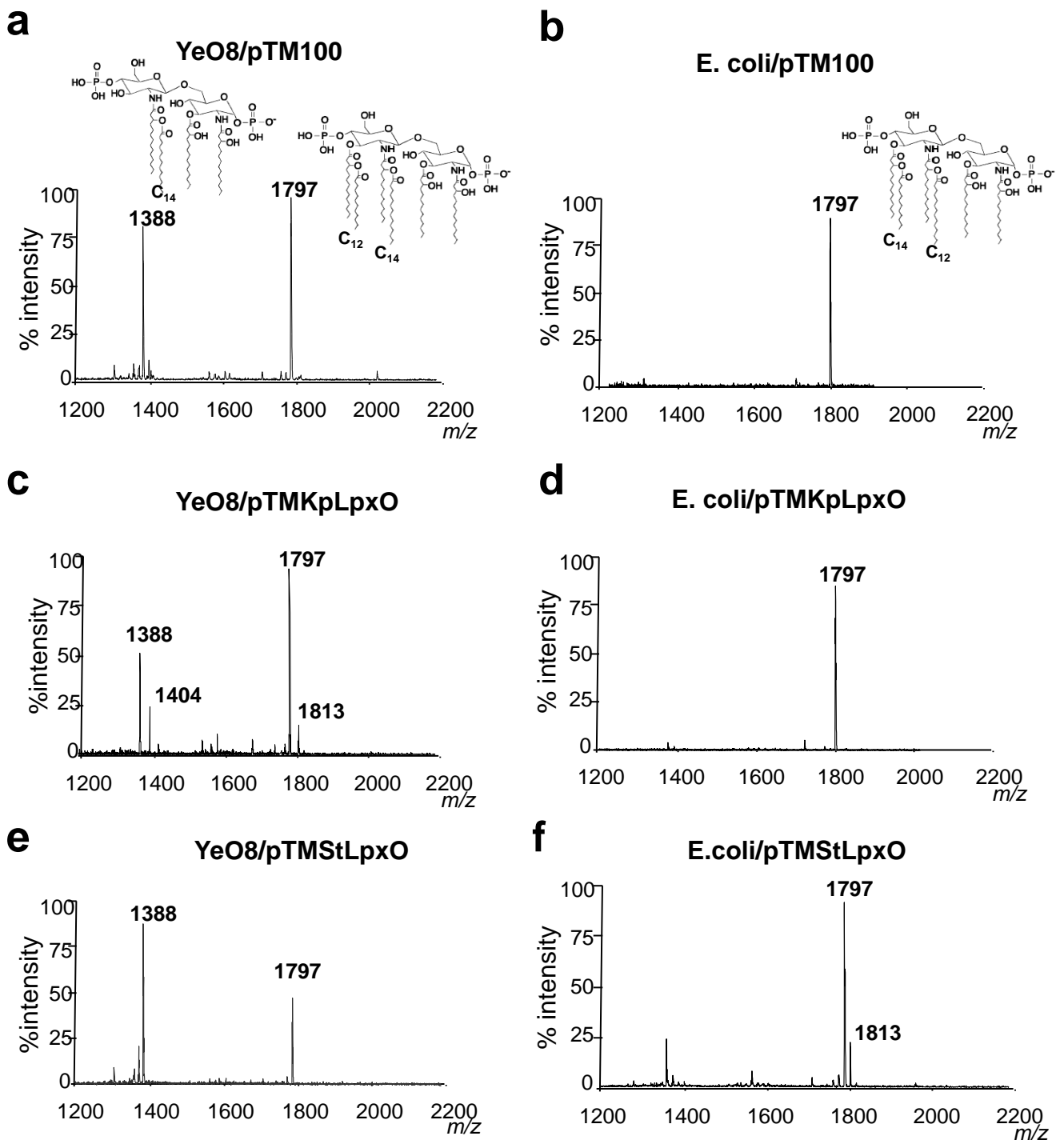
Supplementary Figure 2. Analysis of *K. pneumoniae* *lpxM* mutant lipid A.

Negative ion MALDI-TOF mass spectrometry spectra from **a.** *lpxM* mutant, strain 52145-*lpxMGB*, grown in LB; **b.** lung homogenates of 52145-*lpxMGB* -infected mice after 24 h; **c.** *pagP-lpxM* mutant, strain 52145- Δ *pagP-lpxMGB*, grown in LB. In a and c, results are representative from three independent extractions. In b, results are representative from extractions from five infected animals.



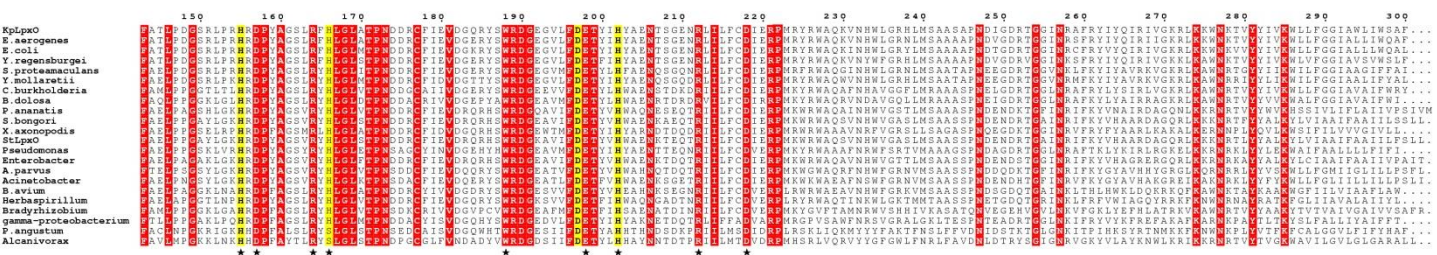
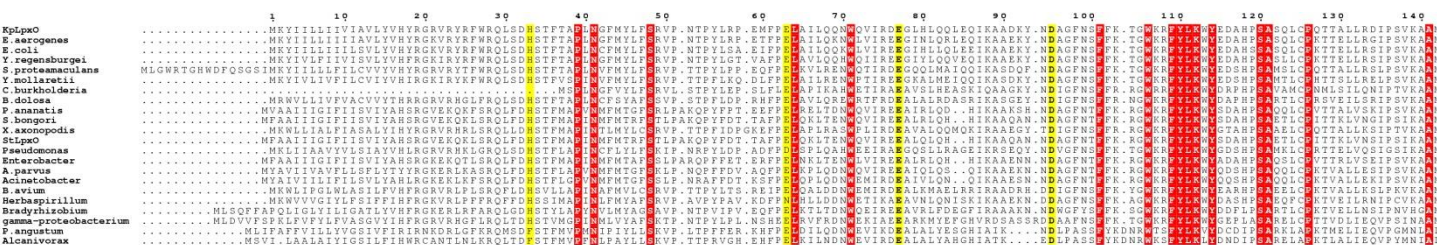
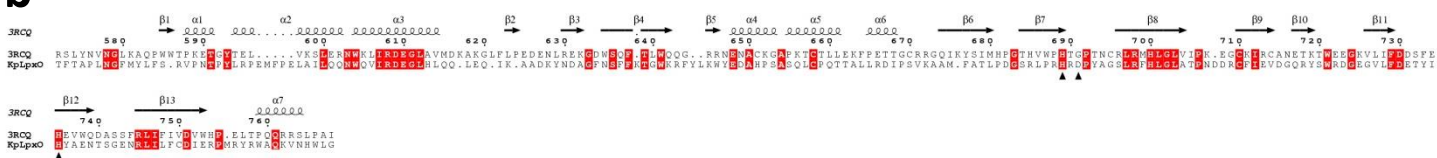
Supplementary Figure 3. *Klebsiella* lipid A plasticity.

Negative ion MALDI-TOF mass spectrometry spectra from **a**. 52145- Δ *IpxOCom* grown in LB. **b** Kp52145 grown in VMM. **c**. 52145-*IpxMGB* grown in VMM. **d**, 52145- Δ *IpxO* grown in VMM. **e**, 52145- Δ *IpxOCom* grown in VMM. In all panels results are representative from three independent extractions.



Supplementary Figure 4. *Klebsiella* LpxO hydroxylates the 2'-linked C₁₄

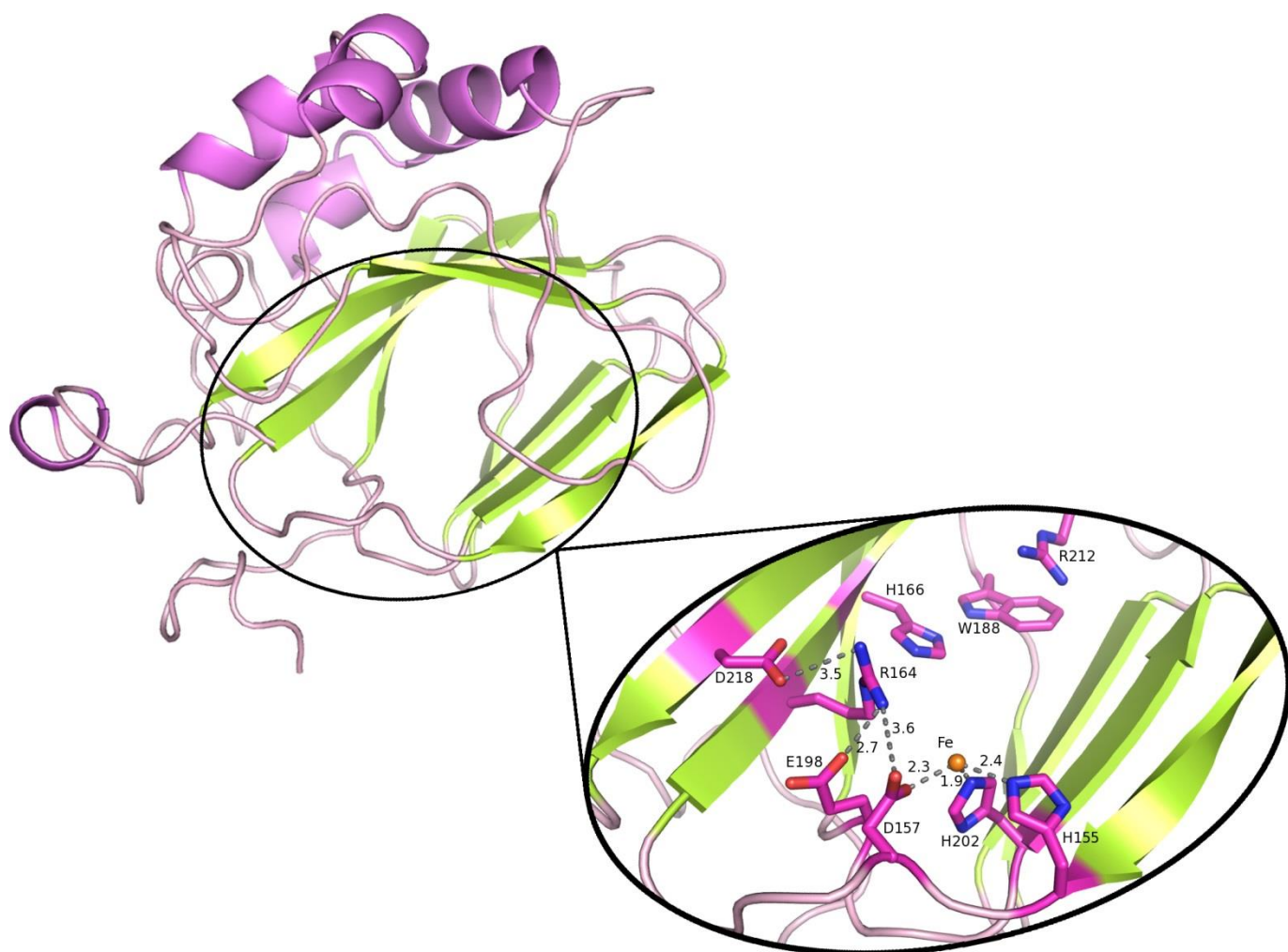
Negative ion MALDI-TOF mass spectrometry spectra from *Y. enterocolitica* O:8 strain grown at 37°C in LB harbouring a. pTM100; c pTMKpLpxO; e, pTMStLpxO plasmids. Negative ion MALDI-TOF mass spectrometry spectra from *E. coli* MG1655 grown at 37°C in LB harbouring b. pTM100; d, pTMKpLpxO; f, pTMStLpxO plasmids. In all panels results are representative from three independent extractions.

a**b**

Supplementary Figure 5. Alignment of *Klebsiella* LpxO homologs.

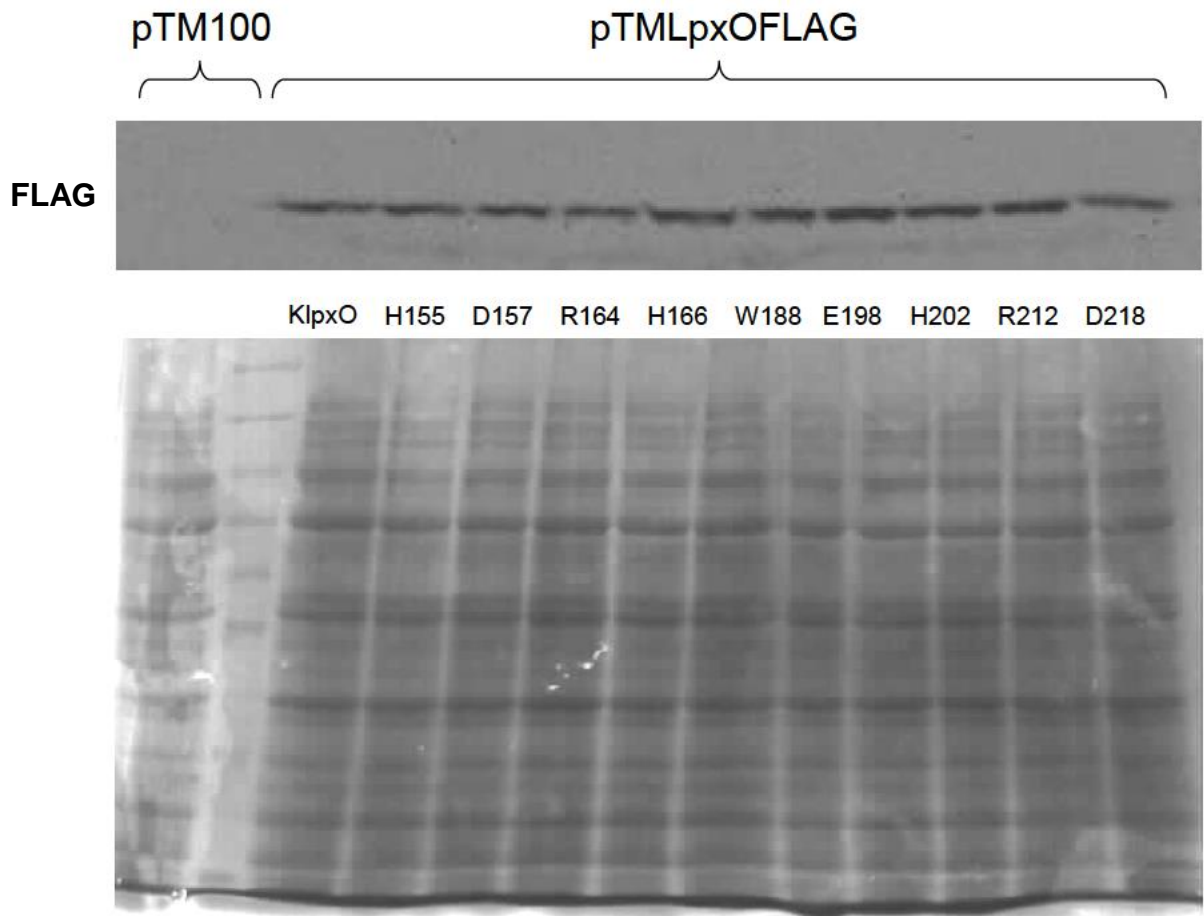
a KpLpxO was aligned with similar sequences (identity ranging from 40 % to 90 %) and the multiple sequence alignment shows a number of conserved residues (red). The residues suggested to be important in bovine Asp/Asn β -hydroxylase and StLpxO (yellow) are conserved in KpLpxO. Black stars indicate the mutated residues in KpLpxO.

b Alignment for modelling. The alignment of KpLpxO with human Asp/Asn β -hydroxylase isoform A (PDB code 3RCQ) shows some conserved residues (red), including the two histidines (H155, H202 [KpLpxO numbering]) in the iron-binding motif (indicated by black triangles). The secondary structure of human Asp/Asn β -hydroxylase is shown above the alignment.

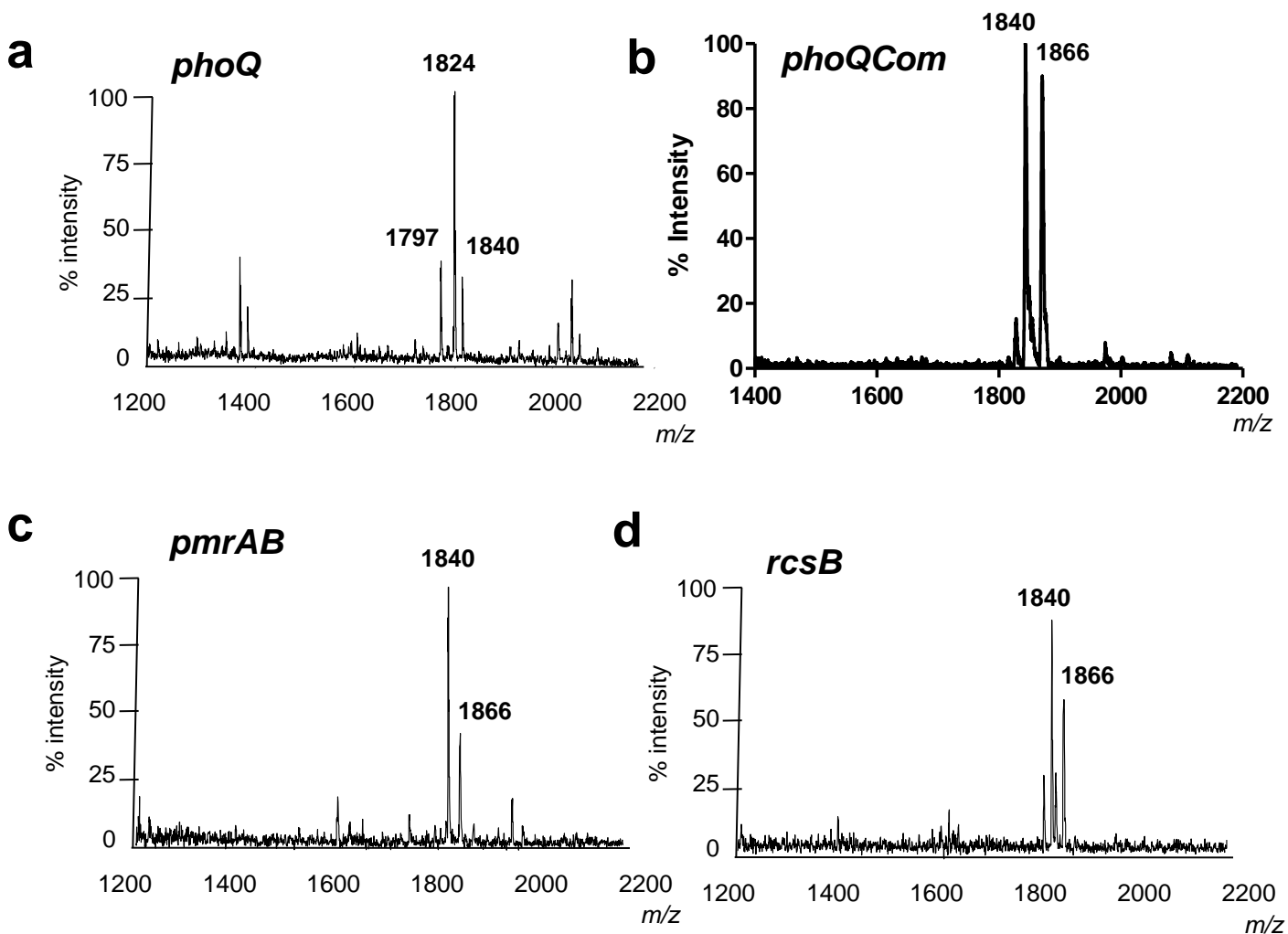


Supplementary Figure 6. 3D model of KpLpxO and mutated amino acids.

KpLpxO is likely to have transmembrane domains in the N- and C-terminus, and a central catalytic domain with the Asp/Asn β -hydroxylase fold (helices shown in violet, β -strands in green, and loops in light pink). The ellipse indicates the active site cavity, which in the magnification shows the mutated amino acids as sticks in pink. The canonical iron-binding motif H155-X-D-X44-H202 is shown with a bound iron (orange sphere) and hydrogen bonds are shown as grey dashes. The hydrogen-bonding network shows that D157, E198, and D218 might be essential for keeping R164 in the right position.

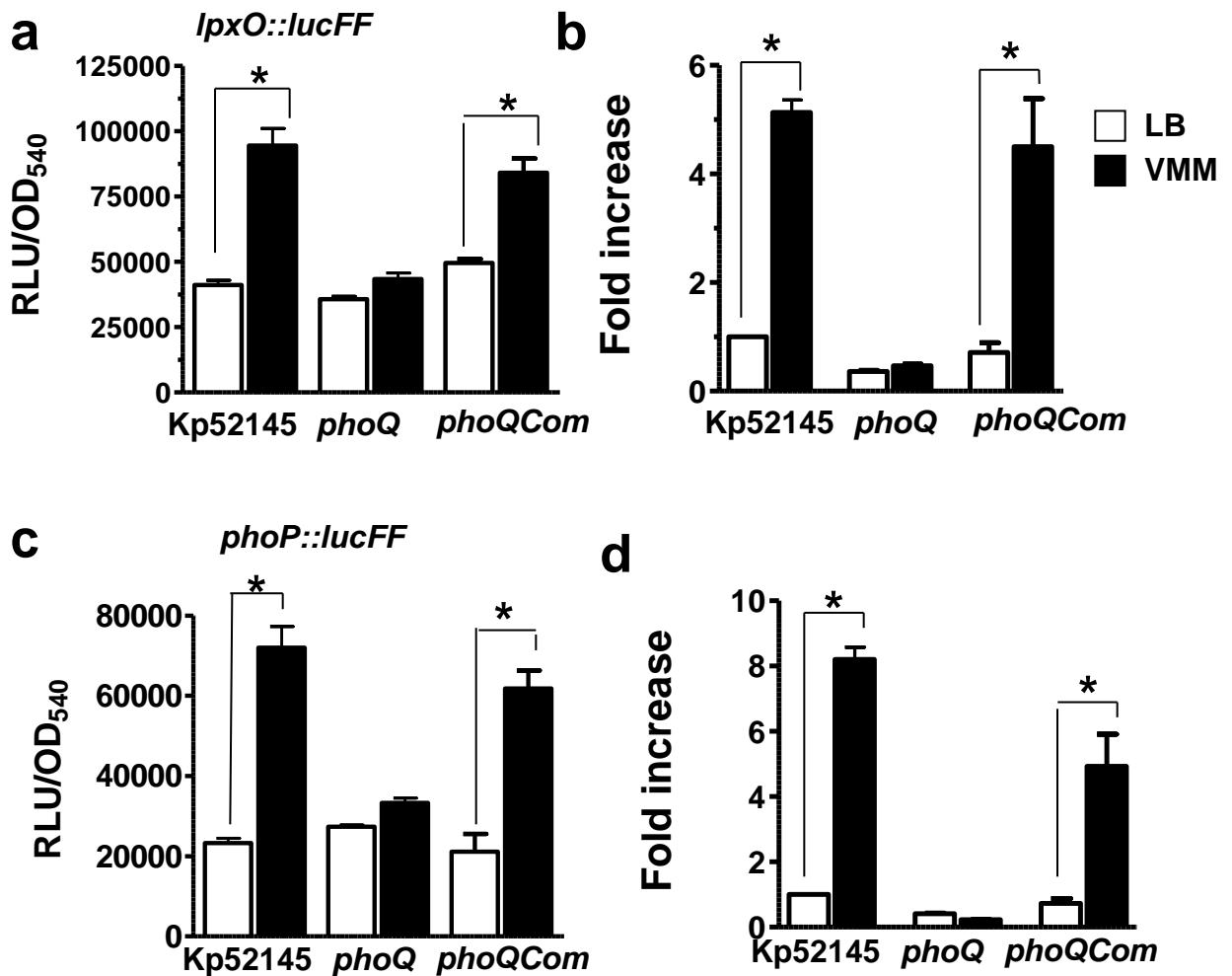


Supplementary Figure 7. Western blot analysis of LpxO FLAG tagged levels.
Upper panel, detection of LpxO FLAG tagged proteins.
Lower panel, Coomassie staining of the SDS-PAGE gel before blotting.



Supplementary Figure 8. PhoPQ two component system controls the lipid A pattern of *K. pneumoniae* cultured in VMM.

Negative ion MALDI-TOF mass spectrometry spectra from **a.**, 52145- Δ *phoQ*GBB (*phoQ*); **b.**, 52145- Δ *phoQ*GBCom (*phoQCom*) **c.**, 52145- Δ *pmrAB* (*pmrAB*); **d.**, 52145- Δ *rcsB* (*rcsB*) grown in VMM. In all panels results are representative from three independent extractions.



Supplementary Figure 9. PhoPQ two component system governs *phoP* and *lpxO* expressions in VMM.

a., Analysis of the expression of *lpxO* by measuring luciferase activity of Kp52145, 52145- Δ *phoQGB* (*phoQ*) or 52145- Δ *phoQGBCom* (*phoQCom*) carrying *lpxO::lucFF* transcriptional fusion. **b.** *lpxO* mRNA levels assessed by RT-qPCR. **c.**, Analysis of the expression of *phoP* by measuring luciferase activity of Kp52145, 52145- Δ *phoQGB* (*phoQ*) or 52145- Δ *phoQGBCom* (*phoQCom*) carrying *phoP::lucFF* transcriptional fusion. **d.** *phoP* mRNA levels assessed by RT-qPCR. In all panels bacteria were grown in LB (white bars) or VMM (black bars). Data are presented as mean \pm SD (n = 3). *, results are significantly different ($P < 0.05$; one-tailed *t* test) from the results for bacteria grown in LB.

Supplementary Table 1. Summary of lipid A species expressed by Kp52145 grown in different media *in vitro* at 37°C.

Results are representative from three independent extractions.

Growth Medium	Observed ion (m/z)	Acyl substitution	Proposed fatty acid, phosphate and carbohydrate composition
LB			
+ 200 uM 2' 2' Dipyriddy disulfide	1404	Tetra-acyl	4x C14:0(3-OH), 2P
	1824	Hexa-acyl	4x C14:0(3-OH), 2x C14:0, 2P
	1850	Hexa-acyl	4x C14:0(3-OH), 1x C14:0, 1x C16:0, 2P
	1955	Hexa-acyl	4x C14:0(3-OH), 2x C14:0, 1x Ara4N, 2P
	2063	Hepta-acyl	4x C14:0(3-OH), 2x C14:0, 1x C16:0, 2P
N minimal medium pH 7.5 (glycerol as carbon source)			
10 mM Mg	1360	Tetra-acyl	3x C14:0(3-OH), 1x C12:0, 2P
	1797	Hexa-acyl	4x C14:0(3-OH), 1x C14:0, 1x C12:0, 2P
	2036	Hepta-acyl	4x C14:0(3-OH), 1x C14:0, 1x C12:0, 1x C16:0, 2P
5 mM Mg	1360	Tetra-acyl	3x C14:0(3-OH), 1x C12:0, 2P
	1797	Hexa-acyl	4x C14:0(3-OH), 1x C14:0, 1x C12:0, 2P
	2036	Hepta-acyl	4x C14:0(3-OH), 1x C14:0, 1x C12:0, 1x C16:0, 2P
10 µM Mg	1797	Hexa-acyl	4x C14:0(3-OH), 1x C14:0, 1x C12:0, 2P
	1824	Hexa-acyl	4x C14:0(3-OH), 2x C14:0, 2P
	1928	Hexa-acyl	4x C14:0(3-OH), 1x C14:0, 1x C12:0, 1x Ara4N, 2P
	2036	Hepta-acyl	4x C14:0(3-OH), 1x C14:0, 1x C12:0, 1x C16:0, 2P
	2063	Hepta-acyl	4x C14:0(3-OH), 2x C14:0, 1x C16:0, 2P
RPMI 1640			
serum free	1824	Hexa-acyl	4x C14:0(3-OH), 2x C14:0, 2P
10% fetal calf serum	1388	Tetra-acyl	3x C14:0(3-OH), 1x C14:0, 2P
	1797	Hexa-acyl	4x C14:0(3-OH), 1x C14:0, 1x C12:0, 2P
	1824	Hexa-acyl	4x C14:0(3-OH), 2x C14:0, 2P
M9 minimal medium (glucose as carbon source)			
10 µM Mg pH 7.0 with 100 mM HEPES	1797	Hexa-acyl	4x C14:0(3-OH), 1x C14:0, 1x C12:0, 2P
	1824	Hexa-acyl	4x C14:0(3-OH), 2x C14:0, 2P
	1850	Hexa-acyl	4x C14:0(3-OH), 1x C14:0, 1x C16:0, 2P
pH 6.5 with 100 mM HEPES	1824	Hexa-acyl	4x C14:0(3-OH), 2x C14:0, 2P
	1840	Hexa-acyl	4x C14:0(3-OH), 1x C14:0, 1x C14:0(3-OH), 2P
	1850	Hexa-acyl	4x C14:0(3-OH), 1x C14:0, 1x C16:0, 2P
	1866	Hexa-acyl	4x C14:0(3-OH), 1x C14:0(3-OH), 1x C16:0, 2P
pH 6.0 with 100 mM HEPES	1797	Hexa-acyl	4x C14:0(3-OH), 1x C14:0, 1x C12:0, 2P
	1824	Hexa-acyl	4x C14:0(3-OH), 2x C14:0, 2P
	1850	Hexa-acyl	4x C14:0(3-OH), 1x C14:0, 1x C16:0, 2P
pH 5.5 with 100 mM MES	1797	Hexa-acyl	4x C14:0(3-OH), 1x C14:0, 1x C12:0, 2P
	1824	Hexa-acyl	4x C14:0(3-OH), 2x C14:0, 2P
	1840	Hexa-acyl	4x C14:0(3-OH), 1x C14:0, 1x C14:0(3-OH), 2P
	1850	Hexa-acyl	4x C14:0(3-OH), 1x C14:0, 1x C16:0, 2P
pH 5.0 with 100 mM MES	1824	Hexa-acyl	4x C14:0(3-OH), 2x C14:0, 2P
	1840	Hexa-acyl	4x C14:0(3-OH), 1x C14:0, 1x C14:0(3-OH), 2P
	1850	Hexa-acyl	4x C14:0(3-OH), 1x C14:0, 1x C16:0, 2P
	1866	Hexa-acyl	4x C14:0(3-OH), 1x C14:0(3-OH), 1x C16:0, 2P
pH 4.5 with 100 mM MES	1840	Hexa-acyl	4x C14:0(3-OH), 1x C14:0, 1x C14:0(3-OH), 2P
	1866	Hexa-acyl	4x C14:0(3-OH), 1x C14:0(3-OH), 1x C16:0, 2P

Supplementary Table 2. Identification of catalytic essential LpxO residues.
Results are representative from three independent extractions.

Lipid A 2-hydroxylation		
	<i>m/z</i>	
Kp52145	1840	1866
<i>lpxO</i>	1824	1850
<i>lpxO</i> complemented	1840	1866
Mutations		
H155A	1824	1850
D157A	1824	1850
H202A	1824	1850
R164A	1824	1850
H166A	1824	1850
W188A	1824	1850
E198A	1824	1850
R212A	1824	1850
D218A	1824	1850

Supplementary Table 3. MIC to colistin for *K. pneumoniae* clinical isolates carbapenem resistant.

* MIC significantly different ($P < 0.01$; one-tailed t test) from MIC for the corresponding wild-type strain. n.c.; mutant not constructed. Experiments were repeated two independent times.

	MIC ($\mu\text{g/ml}$)		
	Wild type	<i>lpxO</i> mutant	<i>lpxO::Tn7lpxO</i>
2608	32	2*	24
2609	32	2*	24
2610	128	4*	96
2611	64	2*	48
2612	32	2*	32
2613	64	4*	32
2614	64	2*	48
2615	< 1	n.c.	-
2616	< 1	n.c.	-
2617	< 1	n.c.	-
2618	< 1	n.c.	-
2619	< 1	n.c.	-
2620	< 1	n.c.	-
2621	2	n.c.	-